The Astrophysical Journal, 638:659–667, 2006 February 20

HEATING COOLING FLOWS WITH WEAK SHOCK WAVES

William G. Mathews,[1] Andreas Faltenbacher,[1] and Fabrizio Brighenti[1,2]
Received 2005 May 11; accepted 2005 October 16

ABSTRACT

The discovery of extended, approximately spherical weak shock waves in the hot intercluster gas in Perseus and Virgo has precipitated the notion that these waves may be the primary heating process that explains why so little gas cools to low temperatures. This type of heating has received additional support from recent gasdynamical models. We show here that outwardly propagating, dissipating waves deposit most of their energy near the center of the cluster atmosphere. Consequently, if the gas is heated by (intermittent) weak shocks for several Gyr, the gas within 30–50 kpc is heated to temperatures that far exceed observed values. This heating can be avoided if dissipating shocks are sufficiently infrequent or weak so as not to be the primary source of global heating. Local PV and viscous heating associated with newly formed X-ray cavities are likely to be small, which is consistent with the low gas temperatures generally observed near the centers of groups and clusters where the cavities are located.

Subject headings: cooling flows — galaxies: active — galaxies: clusters: general — galaxies: elliptical and lenticular, cD — X-rays: galaxies — X-rays: galaxies: clusters

1. INTRODUCTION

Successful gasdynamical models of the hot virialized gas in galaxy groups and clusters must satisfy several cardinal requirements (CRs):

CR1.—The rate that gas cools to low temperatures must be less than ~10% of that predicted by conventional cooling flows, $\dot{M} \sim L_X/(5kT/2\mu m_p)$, where L_X is the bolometric X-ray luminosity and T is the mean gas temperature.

CR2.—The gas temperature profile $T(r)$ must increase from the center out to ~0.1–0.3 of the virial radius; i.e., $T(r)$ must look like a conventional cooling flow.

CR3.—The radial abundance profiles in the hot gas must agree with observation, and in particular a mass 10^8–$10^9\ M_\odot$ of iron should be concentrated within ~100 kpc of the central E or cD galaxy.

CR4.—It is necessary to identify the source of heating that reduces the baryon mass fraction below the cosmic value in clusters/groups with mean temperatures less than about 3 keV.

The first of these requirements is necessitated by the well-documented absence of cooling gas in the X-ray spectra of galaxy groups and clusters (e.g., Peterson et al. 2001; Böhringer et al. 2002). Evidently, some additional source of heating is required. In view of the limited energy available in supernova explosions and the uncertain efficiency of thermal conduction (Voigt & Fabian 2004), it is generally thought that the cluster gas is heated directly or indirectly by jets or energetic outflows originating near supermassive black holes (active galactic nuclei [AGNs]) in the cores of cluster-centered elliptical galaxies. But there is no general consensus regarding the physical processes responsible for the heating or the means by which energy is delivered to gas at large distances from the central AGN. In any case, the X-ray–emitting gas closest to the central AGN must not be strongly heated, since that would violate CR2. Positive temperature gradients within 0.1–$0.3r_{vir}$ are typical among cooling flow clusters and groups (Allen et al. 2001; De Grandi & Molendi 2002), although the temperature profile in a few clusters is more nearly isothermal (e.g., AWM-4; O'Sullivan et al. 2005). Assuming that the hot cluster gas is in approximate hydrostatic equilibrium in a Navarro-Frenk-White (NFW) mass distribution, gasdynamical models that produce correct temperature profiles will also have correct density and entropy profiles.

Except possibly for the very center, the gas-phase iron abundance in groups and clusters generally decreases from about solar to ~0.3 ± 0.1 solar at the outer limit of observations. In cool-core clusters a significant fraction of the total gas-phase iron mass, $M_{Fe} \approx 10^8$–$10^9\ M_\odot$, is concentrated within ~100 kpc of the central E or cD galaxy (De Grandi et al. 2004). Metal abundance gradients in the hot gas retain an integrated record of its past association with stars and supernovae that must be reproduced by any successful model (CR3).

To explore the gasdynamical consequences of heating, Brighenti & Mathews (2002a, 2003) considered a wide variety of ad hoc heating scenarios and described the effect of each on the hot gas over many Gyr. In these models the gas was heated either continuously or intermittently, either symmetrically near the center or at off-center locations. X-ray cavities formed in the heated gas generated weak shock waves similar to those found in Perseus. We concluded at that time that none of the many types of heating scenarios satisfied all cardinal requirements listed above. For example, if the heating is symmetric around the center of the flow at a level sufficient to quench the radiative cooling there, we found that cooling still occurred at larger radii in the flow (violating CR1) or the radial temperature gradients in the heated region were invariably negative (violating CR2). To fully shut down a cooling flow, it is necessary to heat the gas nearly to the ("cooling") radius r_{cool}, the radius at which the gas would cool in ~10^{10} yr or during the cluster lifetime.

One of the principal questions in understanding the long-term evolution of cluster gas is whether mass, as well as energy, must be transported out from the central AGN. To investigate this possibility, we recently considered idealized "circulation flows" in which gas heated near the center is buoyantly transported to large radii in the flow, where it merges with the ambient gas and subsequently flows back in (Mathews et al. 2003, 2004). In these circulation flows gas moves simultaneously in both radial directions—there is no net flow of matter and no radiative

[1] Department of Astronomy and Astrophysics, University of California Observatories/Lick Observatory, University of California, Santa Cruz, CA 95064; mathews@ucolick.org.

[2] Dipartimento di Astronomia, Università di Bologna, via Ranzani 1, Bologna 40127, Italy; brighenti@bo.astro.it.

cooling to low temperatures (satisfying CR1). The dense inflowing gas emits most of the X-ray emission and resembles a traditional cooling flow that fills only a fraction of the available volume. The remaining volume is occupied by outflowing low-density bubbles of heated gas that do not contribute much to the X-ray spectrum. A single-temperature interpretation of the emission from such a flow is dominated by the inflowing gas and resembles a normal cooling flow (satisfying CR2). Furthermore, we showed that successful circulation flows must carry both mass and energy out from the center to approximately the cooling radius. The iron abundance peak that surrounds the central E galaxy is easily explained with circulation flows as the repository of all the iron produced by Type Ia supernovae in the central galaxy over time (satisfying CR3).

Other heating scenarios can also be imagined. In the discussion below we explore the possibility that weak dissipating waves created near the center of the flow propagate throughout the hot gas, globally heating the gas and quenching the radiative cooling to low temperatures.

The deep 200 ks *Chandra* observation of the Perseus Cluster by Fabian et al. (2003) revealed the presence of an ensemble of approximately spherical weak shock waves ("ripples") within about 50 kpc of the center. The Perseus Cluster also contains at least four X-ray cavities (bubbles), all within about 35 kpc of the center of the cluster (Birzan et al. 2004). Forman et al. (2003) describe similar spherical waves at 14, 17, and 37 kpc in the Virgo Cluster. These distant shock ripples are almost certainly created by the slow, intermittent inflation of new bubbles near the central AGN. It is important to recognize that weak shocks are produced even by bubbles that expand subsonically. The ripples observed have progressed about halfway to the cooling radius, which is about 130 kpc in Perseus and 75 kpc in Virgo (Peres et al. 1998), assuming $H_0 = 70$ km s^{-1} Mpc^{-1}.

Fabian et al. (2003) argue that dissipating shocks (ripples) excited by inner bubbles are likely to be the dominant heating mechanism that balances radiative cooling throughout the hot gas. They claim that alternative modes of heating—large numbers of tiny effervescent bubbles (Begelman 2001), major central eruptions (Soker et al. 2001; Kaiser & Binney 2003), or heating near the buoyant bubbles (Churazov et al. 2001, 2002; Quilis et al. 2001; Brüggen et al. 2002; Brüggen 2003; Brüggen & Kaiser 2002)—are less effective within $r_{\rm cool}$ than the quasi-continuous large-scale dissipative heating by shock ripples, which can persist even in those clusters (e.g., A1835) that do not currently have central bubble activity.

The idea that ripple wave heating is dominant has been amplified recently by Clarke et al. (2005), who claim that "these shocks dissipate energy which may be sufficient to balance the effects of radiative cooling in the cluster cores." This conclusion has been strongly advocated by Ruszkowski et al. (2004a, 2004b) and Dalla Vecchia et al. (2004), who argue that the approximately spherical dissipation of large-scale waves is more efficient in globally balancing the radiative losses in cluster gas within $r_{\rm cool}$ than viscous heating associated with the flow just around the X-ray cavities. They also emphasize the importance of AGN intermittency in exciting individual ripple waves.

Even with the best available observations, it is impossible to detect an increase in the gas temperature or thermal energy across individual ripples. The two ripples observed in Perseus, for example, are insufficient to increase the cluster energy (or entropy) enough to shut down the global cooling for many Gyr. Because the amount of energy carried and entropy dissipated by each wave is so small, it is necessary to perform a calculation such as we describe here to test the idea that a large number of ripples sustained over time can provide enough dissipation to stop the cooling—without destroying the temperature profile as observed. We show that wave heating fails because the central regions of the cluster, through which all outgoing waves must pass, receive too much dissipated energy and after a few Gyr become much hotter than the temperature observed.

It is not surprising that Dalla Vecchia et al. (2004) and Ruszkowski et al. (2004a, 2004b) were able to reduce radiative cooling by ripple heating in their multidimensional simulations. To achieve this, it is only necessary to adjust the (highly uncertain) power delivered to the hot gas by the AGN to be comparable to the bolometric X-ray luminosity $L_{\rm X}$. By this ad hoc means radiative cooling can be shut down for a time $\sim t_{\rm cool}(r_{\rm heat})$ within the radius $r_{\rm heat} \leq r_{\rm cool}$, where the AGN energy is deposited by ripple shock waves. However, it is essential to determine whether or not cooling flows can be suppressed by ripple heating over many Gyr and still satisfy the gas temperature profiles generally observed (CR2). This is the question we address here. To establish with certainty that ripple wave dissipation can balance radiative losses in a cooling flow, it is necessary to calculate for times comparable to the relevant cooling time or evolutionary lifetime of the cluster.

1.1. *Viscous Heating by Shocks, Sound Waves, and Turbulence*

There has been some confusion about the magnitude of the viscosity that is required for viscous dissipation to offset radiative losses in the hot gas in groups and clusters. In the absence of magnetic fields, the viscosity $\mu_s = 1.1 \times 10^{-16} T^{5/2}$ g cm^{-1} s^{-1} depends only on the temperature (Braginskii 1958). Viscous heating depends strongly on the local velocity gradient, $\sim \mu (du/dl)^2$ ergs cm^{-3} s^{-3}, where l is a spatial coordinate appropriate to the scale of the region where dissipation occurs. Although viscous dissipation occurs on small spatial scales comparable to the mean free path, it can heat a large volume of gas by the passage of dissipating wave fronts or by widespread turbulence.

X-ray cavities can heat the ambient gas by performing work and creating waves as they are initially formed and by viscous dissipation of turbulence produced by their buoyant motion. Birzan et al. (2004) estimated the PV work done by expanding cavities in the hot gas in 16 galaxy clusters and concluded that "this mechanism alone probably does not provide a general solution to the cooling problem." If X-ray cavities inflate adiabatically into an inviscid gas, an amount of work PV is transferred to the local gas. However, a significant fraction of this work is expended in displacing local gas outward in the cluster potential, but this gas returns to its original radius after the buoyant bubble moves away, performing a nearly equal amount of negative work, $-PV$. Consequently, PV overestimates the total energy received by the ambient gas from the cavities.

The absence of resonance scattering of X-ray lines led Mathews et al. (2001) and Churazov et al. (2004) to suggest considerable subsonic turbulence in the central $\sim$60 kpc of Perseus, but strong, extended turbulence may be inconsistent with steep iron abundance gradients observed in Perseus and many similar clusters (e.g., Fabian et al. 2003). If such turbulent energy exists, the buoyant motions of X-ray cavities are a likely source. It is interesting to compare the rate of viscous dissipation near a cavity moving at $\sim$30 kpc in Perseus ($T \approx 3 \times 10^7$ K; $n_e \approx 0.03$ cm^{-3}) to the local volume radiative emissivity. The drag force on a bubble (cavity) of radius r_b moving at velocity u_b is $F_d = \delta_b \rho u_b^2 \pi r_b^2$, where $\delta_b < 1$ is the drag coefficient. If the power expended against drag by a single bubble is $F_d u_b$, the total power within radius r in the flow is $\delta_b \rho u_b^3 \pi r^2 f_a^2$, where $f_a = N_b \pi r_b^2 / 4\pi r^2 < 1$ is the area filling factor for N_b bubbles at radius r in the flow. The total power

deposited in volume $4\pi r^3/3$, $(3/4)\delta_b \rho u_b^3 f_a^2/r$, is ultimately dissipated by viscosity at a rate

$$\dot{\varepsilon}_{\rm visc} = \delta_b \mathcal{M}^3 f_a^2 \frac{3}{4}\frac{\rho c_s^3}{r} = 2.6\times10^{-25}\delta_b \mathcal{M}^3 f_a^2 \times \left(\frac{T}{3\times10^7\ {\rm K}}\right)^{3/2}\left(\frac{n_e}{0.03\ {\rm cm^{-3}}}\right)\left(\frac{r}{30\ {\rm kpc}}\right)^{-1}\frac{\rm ergs}{\rm cm^3\ s},$$

where we assume that the bubbles move subsonically, i.e., $\mathcal{M} = u_b/c_s < 1$, where $c_s = (\gamma kT/0.61 m_p)^{1/2}$ is the sound speed. Note that the absolute value of the viscosity determines the small scales of energy dissipation, but not the amount of turbulent energy dissipated. The rate that energy is radiated at this radius is

$$\dot{\varepsilon}_{\rm rad} = \left(\frac{\rho}{m_p}\right)^2 \Lambda(T,z) \approx 2.4\times10^{-26} \times \left(\frac{n_e}{0.03\ {\rm cm^{-3}}}\right)^2\left(\frac{\Lambda}{2\times10^{-23}}\right)\frac{\rm ergs}{\rm cm^3\ s}.$$

Since we expect $\delta_b \mathcal{M}^3 f_a^2 \ll 1$, the turbulent viscous dissipation directly associated with bubble buoyancy is unlikely to equal the local radiative losses.

Viscous dissipation $\mu(du/dl)^2$ and heating can also be important in large-amplitude sound waves and weak shock waves and must be investigated as a possible means of heating cluster gas. When ripple waves were discovered in Perseus and Virgo, it was assumed that they were weak shocks of the sort that accompanies the creation of X-ray cavities (e.g., Brighenti & Mathews 2002b). Recently, Fabian et al. (2005) propose that cluster gas can be heated by linear sound waves of frequency $f \sim (3\times10^5\ {\rm yr})^{-1}$ that dissipate on scales

$$l_{\rm diss} = \frac{2\rho c_s^3}{(4\mu/3)}\frac{1}{(2\pi f)^2} \sim 50\ {\rm kpc}.$$

Fabian et al. (2005) show that it is possible to approximately offset radiative cooling in large clusters if the wave frequency is sufficiently high and the sound wave luminosity at this frequency is sufficiently large. The low-amplitude linear waves required for this type of heating probably cannot be detected by X-ray observations. By comparison, in shock waves the dissipation occurs over a few mean free paths regardless of the magnitude of the viscosity; i.e., unlike linear wave dissipation, the shock jump conditions and entropy increase do not explicitly depend on the viscosity.

An important question that has not been thoroughly considered is the competition between the viscous dissipation of large-amplitude sound waves as they decay with no change in the waveform and the progressive steepening of the wave profile that results in a shock wave. The dimensionless ratio that determines these quite different evolutionary changes in the waveform is the Goldberg number

$$\Gamma = \frac{(\gamma+1)\mathcal{M}/2}{\ell_{\rm diss}^{-1}/k},$$

where $\delta u = \mathcal{M} c_s$ is the velocity amplitude of the wave and $k = 2\pi/\lambda$ (e.g., Kinsler et al. 2000). The dimensionless Goldberg number is the ratio of $\mathcal{M}$, an indicator of the degree of nonlinearity in the wave, to $l_{\rm diss}^{-1}/k$, the amplitude attenuation over one wavelength at the fundamental frequency of the waveform. The evolution of waves created by X-ray cavities in the Perseus Cluster with period T_p can be estimated by combining the various expressions above,

$$\Gamma = 350\frac{\mathcal{M}}{f_\mu}\left(\frac{n_e}{0.03\ {\rm cm^{-3}}}\right)\left(\frac{T_p}{3\times10^7\ {\rm yr}}\right)^3 \times\left(\frac{3\times10^7\ {\rm K}}{T}\right),$$

where $f_\mu = \mu/\mu_s \lesssim 0.2$ is the deviation of the viscosity from the Braginskii-Spitzer value. Since $\mathcal{M}$ is less than (but comparable to) unity for subsonically expanding cavities, it is obvious that $\Gamma \gg 1$, so the waves created by expanding X-ray bubbles must steepen rapidly into weak shocks.

1.2. *Density Profile and Shock Wave Dissipation*

We describe below how hot cluster gas is heated by dissipating waves created near the central AGN. Since the gas density in groups and clusters varies less steeply than $\rho \propto r^{-2}$, expanding ripple waves created in the bubble region ($\sim$10–20 kpc) lose amplitude as they encounter an increasing mass per unit area; this loss in wave amplitude occurs in addition to viscous dissipation. We wish to determine whether the temperature profiles typically observed in clusters are consistent with ripple shock heating to radius $r_{\rm heat}$ where $t_{\rm cool}(r_{\rm heat})$ is comparable to the likely age of the cluster. Specifically, we study wave dissipation in the Perseus Cluster, where weak ripple shocks are well documented by observation. We begin with a discussion of the properties of this cluster.

2. THE PERSEUS CLUSTER

Churazov et al. (2004) give analytic fits to the density and temperature profiles in Perseus at the spatial resolution of their *XMM-Newton* observations. The deep *Chandra* observation of Perseus by Sanders et al. (2004) is consistent with the same temperature profile as given in Churazov et al. (2004),

$$T = 8.12\times10^7\frac{1+(r/71)^3}{2.3+(r/71)^3}\ {\rm K}, \quad (1)$$

where r is in kpc, with a distance determined with $H_0 = 70\ {\rm km\ s^{-1}\ Mpc^{-1}}$.

The azimuthally averaged density profile in Perseus is given by

$$n_e(r) = \frac{0.0192}{1+(r/18)^3} + \frac{0.046}{[1+(r/57)^2]^{1.8}} + \frac{0.0048}{[1+(r/200)^2]^{0.87}}\ {\rm cm^{-3}}. \quad (2)$$

The last two terms are taken from Churazov et al. (2004), and the first term corrects for the *Chandra* observations of Sanders et al. (2004) in the high-density core.

The acceleration of gravity $g(r)$ in the Perseus Cluster can be found by assuming hydrostatic equilibrium in the hot gas and differentiating the equations above,

$$g_{nT}(r) = -\frac{kT}{\mu m_p}\left(\frac{1}{n_e}\frac{dn_e}{dr} + \frac{1}{T}\frac{dT}{dr}\right), \quad (3)$$

and this is shown with the dot-dashed line in Figure 1. Within about 10 kpc the observed acceleration $g_{nT}(r)$, decreases, since $T(r)$ and $n_e(r)$ in equations (1) and (2) become constant as $r \to 0$. A centrally decreasing gravitational acceleration is clearly inconsistent with the expected dark and luminous mass distributions in

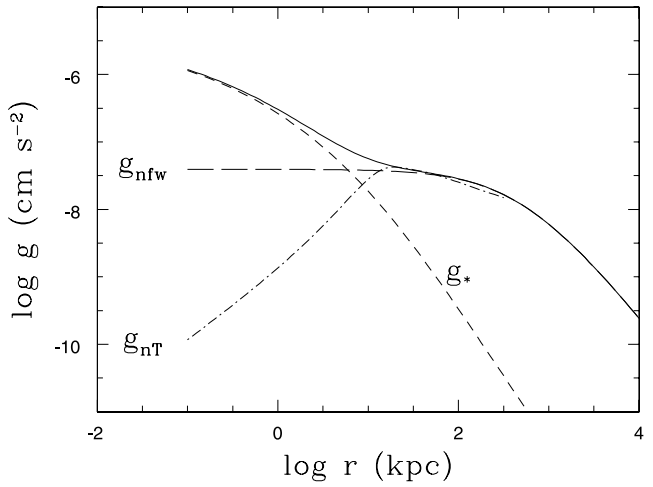

FIG. 1.—Acceleration of gravity in the Perseus Cluster. The quantity g_{nT} is derived from the observed gas density and temperature (*dot-dashed line*); the $g_{\rm NFW}$ component, from the dark halo (*long-dashed line*); and the g_* component, from stars in the central galaxy NGC 1275 (*short-dashed line*); and $g = g_{\rm NFW} + g_*$ is the total adopted acceleration (*solid line*).

this region. The azimuthally (i.e., spherically) averaged fitting functions for $n_e(r)$ and $T(r)$ fail for $r \lesssim 10$ kpc, since this is the region occupied by large X-ray cavities. Even if the gas is close to hydrostatic equilibrium everywhere, as we believe to be the case, azimuthal averaging underestimates n_e and $d\log n_e/dr$ in the high-density intercavity gas that produces most of the X-ray emission. Although the drop in $g_{nT}(r)$ within 10 kpc is unphysical, in the region 10 kpc $\lesssim r \lesssim 300$ kpc, where both $n_e(r)$ and $T(r)$ are observed, g_{nT} should accurately measure the Perseus gravitational field.

We match the observed $g_{nT}(r)$ by combining an NFW dark halo and a stellar contribution from the cluster-centered galaxy NGC 1275, $g = g_{\rm NFW} + g_*$. The halo acceleration is simply

$$g_{\rm NFW} = \frac{GM_{\rm vir}}{r^2}\frac{\log(1+y) - y/(1+y)}{\log(1+c) - c/(1+c)}, \tag{4}$$

where $y = cr/r_{\rm vir}$, c is the concentration, and r is the radius in kpc. The acceleration $g_{\rm NFW}(r)$, determined with the parameters $M_{\rm vir} = 8.5\times10^{14}\ M_\odot$, $r_{\rm vir} = 2.440$ Mpc, and $c = 6.81$ and shown as a long-dashed line in Figure 1, is a reasonably good fit to $g_{nT}(r)$ at 10 kpc $\lesssim r \lesssim 300$ kpc.

The physical properties of the central galaxy in Perseus, NGC 1275, are problematical, since it appears to be an elliptical galaxy that has experienced a recent merger, perhaps with a smaller spiral galaxy (Conselice et al. 2001). The global color of NGC 1275, $(B-V)_0 = 0.72 \pm 0.03$, is significantly bluer than a normal E galaxy, but the stellar surface brightness profile follows a de Vaucouleurs $R^{1/4}$ law to at least 150 kpc (Prestwich et al. 1997). We therefore assume here that the stellar mass of NGC 1275 is dominated by an old stellar population, as in normal E galaxies, intermixed with an additional population of young, luminous stars that does not contribute significantly to the total mass. The stellar mass distribution $M_*(r)$ and $g_*(r)$ for a de Vaucouleurs profile can be found from the effective radius, the total luminosity L_B of *old* stars, and the stellar mass-to-light ratio M/L_B. At a distance of 73.4 Mpc the effective radius of NGC 1275 is $R_e = 6.41$ kpc (RC3). The total magnitude $M_V = -21.62$ of the old stars can be found from the stellar velocity dispersion $\log\sigma_* = 2.40$ (Bettoni et al. 2003) using the $\log\sigma_* - M_V$ correlation from Faber et al. (1997). If $B-V = 0.95$, as in normal E galaxies with old stellar populations, then $M_B = -20.67$ and $L_B = 2.70\times10^{10}L_{B\odot}$, and we ignore the mass and luminosity of recently formed stars. For this L_B we find $M/L_B = 9.0$ from Trujillo et al. (2004), so the total stellar mass of NGC 1275 is $M_{*t} = 2.43\times10^{11}\ M_\odot$. The stellar acceleration $g_*(r) = GM_*(r)/r^2$ for a de Vaucouleurs profile, shown as the short-dashed line in Figure 1, can be accurately fit with

$$g_*(r) = \left[\left(\frac{r^{0.5975}}{3.206\times10^{-7}}\right)^s + \left(\frac{r^{1.849}}{1.861\times10^{-6}}\right)^s\right]^{-1/s}$$

in cgs with $s = 0.9$ and r in kpc. We neglect the self-gravity of the hot gas. The total two-component acceleration $g(r) = g_{\rm NFW} + g_*$, shown as a solid line in Figure 1, fits $g_{nT}(r)$ quite well for $r \gtrsim 10$ kpc.

3. EXCITING WAVES

We wish to generate spherical shock waves of low amplitude that propagate out through the Perseus gas. The objective is to determine whether this type of shock heating (dissipation) can provide enough energy to the cluster gas to shut down the cooling for times $\sim$4 Gyr comparable to the likely age of the cluster and still preserve the observed temperature profile. Waves can be generated with a sinusoidally oscillating piston located in the bubble region. To create such a AGN wave machine, it is convenient to use Lagrangian, rather than the usual Eulerian, hydrodynamics, since the boundary condition at the piston is more straightforward. The equation of motion is

$$\frac{\partial u}{\partial t} = -\frac{1}{\rho}\frac{\partial}{\partial r}(P+Q) - g, \tag{5}$$

where

$$u = \frac{\partial r}{\partial t} \tag{6}$$

is the velocity defined in terms of the local Eulerian radius r. The equation of continuity is simply

$$\rho\Delta(4\pi r^3/3) = \Delta m, \tag{7}$$

where $\Delta(4\pi r^3/3)$ is the volume of computational zones of mass Δm. The thermal energy equation with radiative losses is

$$\frac{\partial\varepsilon}{\partial t} = \frac{P+Q}{\rho^2}\frac{\partial\rho}{\partial t} - \left(\frac{\rho}{m_p}\right)^2\Lambda(T,z), \tag{8}$$

where $\varepsilon = 3P/2\rho$ is the specific thermal energy and $z \approx 0.4$ is the metal abundance in solar units. The artificial viscosity

$$Q = a^2\rho(\Delta u)^2 \tag{9}$$

depends on the velocity difference Δu across the computational zones and a dimensionless coefficient a of order unity to smooth the postshock flow. The artificial viscosity ensures that the correct dissipative heating in the shock occurs over several computational zones.

Spherical ripple waves can be generated by requiring that the inner boundary $r_p(t)$ of the innermost computational zone, initially at r_{p0}, oscillates with amplitude Δr_p and period T_p,

$$r_p = r_{p0} + \Delta r_p \sin(2\pi t/T_p), \tag{10}$$

with velocity

$$u_p = (2\pi\Delta r_p/T_p)\cos(2\pi t/T_p).$$

Gas within the initial piston radius r_{p0} does not participate in the flow—this is reasonable, since we are interested in heating the much larger volume of gas between the 10–30 kpc region, where the cavities are observed, and the distant cooling radius, $r_{\rm cool} \approx 130$ kpc. The total mechanical energy delivered to the gas by the piston after time t is

$$E_m(t) = \int_0^t 4\pi r_p^2 P_p u_p\, dt, \tag{11}$$

where $P_p(t)$ is the instantaneous gas pressure at $r_p(t)$. If P_p were constant, then no mechanical luminosity (power) is delivered to the gas in one cycle,

$$\langle L_m\rangle_{\rm cy} = \langle dE_m/dt\rangle_{\rm cy} = \frac{8\pi^2 r_{p0}^2 \Delta r_p P_p}{T_p}\int_0^{2\pi}[1+(\Delta r_p/r_{p0})\sin\tau]^2\cos\tau\, d\tau = 0.$$

The mechanical luminosity depends critically on the asymmetry in the gas pressure at the piston $P_p(t)$, which is significantly larger when the piston moves outward, compressing the local gas, than when it recedes inward. Nevertheless, in general we expect $L_m \propto r_{p0}^2\Delta r_p/T_p \propto r_{p0}^2|u_p|$. The piston parameters—$r_{p0}$, Δr_p, and T_p—can be selected by choosing $T_p \sim 10^7$–10^8 yr, as expected for the AGN periodicity from many observations, and then selecting Δr_p so that the peak piston velocity $|u_p| = 2\pi\Delta r_p/T_p$ remains subsonic, since strong shocks are not observed around the X-ray cavities. Finally, r_{p0} can be increased until $\langle L_m\rangle$ is comparable to the bolometric luminosity $L_{\rm X}$, a necessary condition to quench the cooling flow. Alternatively, we can compare $E_m(t)$ with the total energy radiated after time t,

$$E_{\rm rad}(t) = \int_0^t dt \int_V (\rho/m_p)^2\Lambda(T,z)\, dV,$$

where V is the total computational volume.

4. A PURE COOLING FLOW IN PERSEUS

Before considering the heating effects of outwardly propagating waves, it is useful to calculate a pure cooling flow in the Perseus Cluster environment. This can be accomplished by fixing the piston at some small radius $r_{p0} = 1$ kpc and setting $\Delta r_p = 0$. In our solutions of the Lagrangian equations we begin with a configuration that is in strict hydrostatic equilibrium, which is probably an excellent approximation outside the bubble region and a good approximation even near the center, where the gas velocities are largely subsonic. Initial hydrostatic equilibrium is enforced on the computational grid by demanding that the differenced form of equation (5) correspond to zero velocity, $u_j = 0$, at all zone boundaries r_j,

$$g_j = -\frac{1}{0.5(\rho_{j+1/2}+\rho_{j-1/2})} \times \frac{k}{\mu m_p}\frac{(\rho_{j+1/2}T_{j+1/2}-\rho_{j-1/2}T_{j-1/2})}{0.5(r_{j+1}-r_{j-1})}. \tag{12}$$

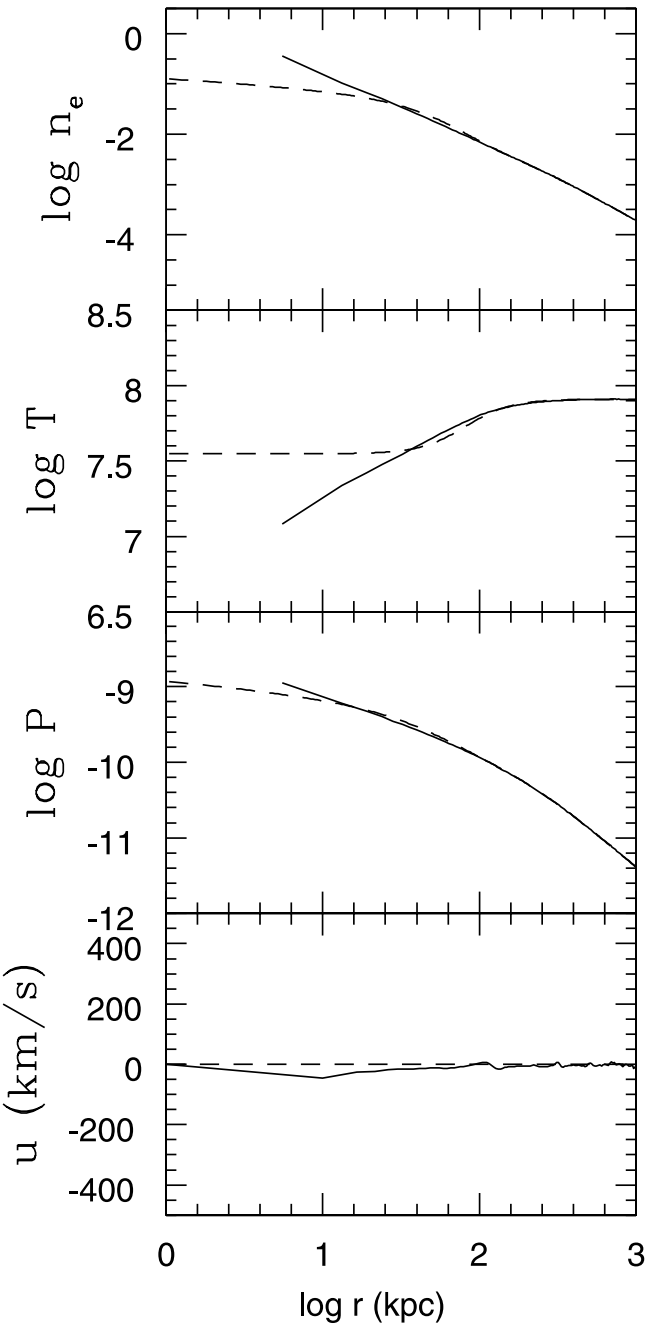

FIG. 2.—Standard cooling flow in the Perseus Cluster after 4 Gyr (*solid lines*) overplotted with the observed gas density (*top; dashed line*), temperature (*second from top; dashed line*), pressure (*third from top; dashed line*) and initial velocity (*bottom; dashed line*).

The gravitational acceleration at every zone boundary is $g_j = g(r_j)$, where $g(r)$ is plotted in Figure 1 with a solid line. The observed temperature profile is insensitive to the volume filling factor in the bubble region (Mathews et al. 2004) and *Chandra* and *XMM-Newton* observations are consistent with the same $T(r)$, so it is natural to assume $T_{j+1/2} = T(r_{j+1/2})$, using the analytical fit to the observed temperature profile described previously. With these assumptions, the difference equation above can be solved recursively for $\rho_{j+1/2}$ from the innermost zone outward. If necessary, the density of the innermost zone is adjusted slightly so that the overall density profile agrees with that described by equation (2). In general, the initial gas density $\rho_{j+1/2}$ within $r \sim 10$ kpc, which corresponds to the intercavity density, is somewhat larger

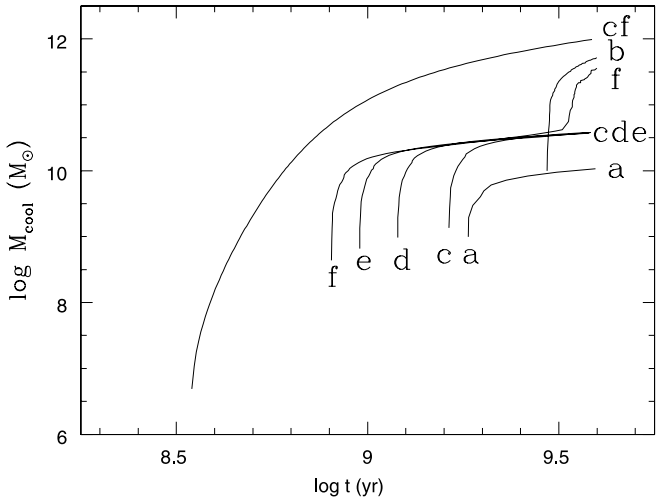

FIG. 3.—Total mass of gas in $M_\odot$ that cooled after time t in the cooling flow (model cf) and in six flows with ripple shock heating, models a → f.

than the analytic fit (eq. [2]), which is a spherical average including both cavity and intercavity gas.

As gas radiates and flows toward the center in a normal cooling flow, the density rises until radiative cooling eventually becomes catastrophic. When the gas temperature in a Lagrangian zone drops below 3×10^5 K, the zone becomes spatially very narrow, and we remove it from the calculation, filling its small volume with a small amount of gas from neighboring zones. Since the inner boundary at $r_{p0} = 1$ kpc is stationary, all the gas cools just beyond that small radius. A shock near r_{p0} prevents the inflowing gas from attaining large negative velocities.

The solid lines in Figure 2 show the cooling flow after 4 Gyr compared to the initial profiles shown as dashed lines. We select 4 Gyr (redshift $z \sim 0.5$), since massive clusters such as Perseus may have evolved significantly over longer times. Toward the center of the flow the computed gas density n_e rises above the observations in $r \lesssim 20$ kpc as $r \rightarrow r_{p0}$; such a density rise is typical in traditional cooling flows (see, e.g., Mathews & Brighenti 2003) and is enhanced further in Perseus by the central X-ray cavities that lower the mean observed density. By 4 Gyr the gas cooling rate shown in Figure 3 has stabilized at $\dot{M} = 250\ M_\odot\ \mathrm{yr}^{-1}$, and the huge total mass of cooled gas at the center, $M_{\rm cool} = 9.8 \times 10^{11}\ M_\odot$, is equal to all the gas within 73 kpc in the initial configuration. Our $\dot{M}$ is nearly identical to the cooling flow rate for Perseus predicted by Sanders et al. (2004), $\dot{M} \approx 255\ M_\odot\ \mathrm{yr}^{-1}$, but is inconsistent with their *Chandra* observations that show no evidence that gas is cooling below $\sim 2 \times 10^7$ K. Heating by ripple wave dissipation or other means is necessary to prevent this cooling.

We have advocated that gas near the centers of cooling flows is heated and buoyantly recirculated to large radii extending to $\sim r_{\rm cool}$ (Mathews et al. 2003, 2004). In these circulation flows both mass and energy are transported outward, but the thermal profile of the flow is nearly identical to that of a normal cooling flow; i.e., $T(r)$ is insensitive to the radial variation of the volume filling factor occupied by the rising cavities (bubbles) as shown by Mathews et al. (2004). For this reason it is noteworthy in Figure 2 that the computed cooling flow temperature profile after 4 Gyr is almost identical to the observed profile for $r \gtrsim 30$ kpc. Since a pure cooling inflow matches the observed temperature and density in this outer region of Perseus so well, we infer that there is no need for conductive heat transport in this region of the flow, although some modest heating may occur. In § 5 we explore whether this radiative cooling in the Perseus Cluster, $\dot{M} = 250\ M_\odot\ \mathrm{yr}^{-1}$, can be significantly reduced by dissipative losses in outwardly propagating weak shock waves (ripples).

5. RIPPLE-HEATED FLOWS

To create a series of outwardly propagating weak shock waves that move out into the Perseus atmosphere, we allow the spherical piston at radius r_{p0} to undergo sinusoidal oscillations with amplitude Δr_p and period T_p. Since strong shocks are rarely observed surrounding X-ray cavities, we select parameters for which the maximum velocity of the piston $|u_{p,\max}| = 2\pi\Delta r_p/T_p$ is less than the sound speed in the local hot gas, $c_s(r_p) = [5kT(r_p)/3\mu m_p]^{1/2} = 958[T(r_p)/3 \times 10^7\ \mathrm{K}]^{1/2}$ km s^{-1}. Note that weak shocks are created even when $|u_p| < c_s$.

The flows with piston parameters listed in Table 1 are a representative sample of our exploration of heating by dissipating ripple waves. The first flow of this type is shown in Figure 4 at two times, designated "a1" after 4×10^7 yr and "a" after 4 Gyr. If the gas density varied as $\rho \propto r^{-2}$, outwardly propagating dissipationless waves would encounter nearly the same mass per unit area at every radius and their amplitude would remain unchanged. However, in Perseus the density drops slower than $\rho \propto r^{-1.6}$, so the wave amplitude is expected to decrease with radius as a larger mass participates in the waves. This is seen most clearly in the gas velocity panel in Figure 4 for model a. The piston parameters of model a have been selected so that the mechanical energy $E_m(t)$ expended by time t is initially slightly larger than the radiated energy, as illustrated in Figure 5—this requires a piston velocity $|u_p|$ that is a large fraction of the initial sound speed. As can be seen in Figure 3, the total mass of cooled gas in model a is small, and this cooling occurs close to the piston. Nevertheless, this solution is clearly unacceptable because it has the wrong density and temperature profiles. As expected, most of the wave dissipation occurs at small radii in the flow, resulting in temperatures exceeding 10^8 K, with negative dT/dr continuing to nearly the cooling radius. The view of model a at an earlier time in the first column of Figure 4 (model a1) shows that rather strong shocks were present at early times. By 4 Gyr these shocks produced the heating shown in the second column (model a). After the central regions in Perseus have been heated to these unrealistically high temperatures, the piston produces a more rounded innermost wave profile in flow a, a subsonic nonlinear wave that shocks farther out.

In model b we consider a flow with the same velocity u_p as in model a, but with a shorter period, $T_p = 10^7$ yr, and the resulting flow has an entirely different character. The outer part of flow b beyond 50 kpc in Figure 4 is essentially a cooling inflow, and this is verified in the bottom panel, where $\langle u \rangle < 0$. The cooling rate and total cooled gas in model b are unacceptably large (Fig. 3).

TABLE 1
PISTON PARAMETERS TO CREATE SHOCK RIPPLES

Model	$t_{\rm comp}$[a] (Gyr)	r_p (kpc)	Δr_p (kpc)	T_p (yr)	u_p (km s^{-1})	$r_p^2\lvert u_p\rvert$ (kpc^2 km s^{-1})
a1.....	0.04	23.8	3.9	3×10^7	800	4.5×10^5
a.....	4	23.8	3.9	3×10^7	800	4.5×10^5
b.....	4	23.8	1.3	1×10^7	800	4.5×10^5
c.....	4	31.5	2.23	3×10^7	457	4.5×10^5
d.....	4	23.8	2.23	3×10^7	457	2.6×10^5
e.....	4	18.1	2.23	3×10^7	457	1.5×10^5
f.....	4	13.8	2.23	3×10^7	457	0.87×10^5

[a] Total time of flow calculation.

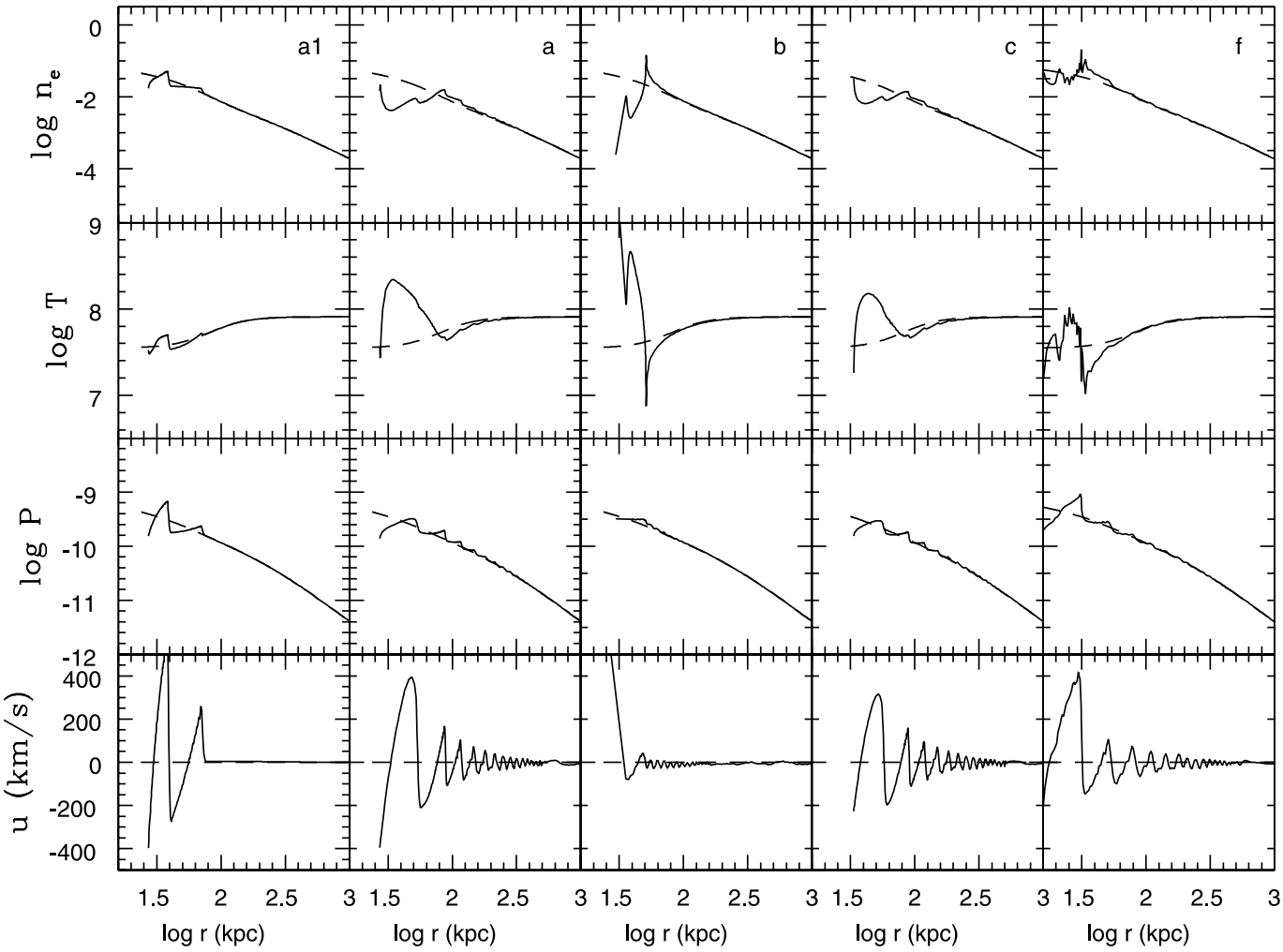

FIG. 4.—Computed gas density, temperature, pressure, and velocity after 4 Gyr in models a–c and f (*solid lines*) compared with the observed (or initial) profiles (*dashed lines*).

All of this cooling occurs at $r \approx 50$ kpc, where the gas temperature has a sharp minimum and the density has a corresponding rise. The waves generated by the piston are unable to penetrate the impedance barrier at $r \approx 50$ kpc, and this accounts for the very low wave amplitude at larger r. Within $r \approx 50$ kpc the dissipating waves reflect back and forth, raising the gas temperature far above that observed in Perseus.

In models c–f the piston amplitude Δr_p and period T_p are chosen so that the piston velocity u_p is more subsonic than in the previous solutions (Table 1). As we have discussed already, to achieve an approximate balance between mechanical and radiative luminosity when u_p is smaller, it is necessary to increase the mean piston position r_{p0}. In model c the piston position $r_{p0} = 31.5$ kpc is near the outer limits of the observed X-ray cavities in Perseus. In Figure 5 it is seen that E_m is only slightly less than $E_{\rm rad}$ during the entire calculation to 4 Gyr, but Figure 3 shows that very little gas (all near the piston) has cooled. However, as with model a, the gas temperature in the region 37 kpc $\lesssim r \lesssim$ 57 kpc of model c exceeds 10^8 K, which is far in excess of the temperature observed in Perseus.

Finally, we consider a series of models, d–f, in which u_p remains fixed at the small value in model c, but r_{p0} is slowly reduced. A smaller mean piston radius r_{p0} is expected to result in lower mechanical energy input $E_m \propto r_{p0}^2 |u_p|$ relative to the total radiated energy $E_{\rm rad}$. This increasing discrepancy can be seen by comparing models c and f in Figure 5. The overall character of solutions c $\rightarrow$ e remains about the same, with a small amount of cooling (Fig. 3), but with temperature profiles that peak at small radii and therefore are inconsistent with the observations. Finally, in model f the mechanical energy is unable to keep large amounts of gas from cooling (Fig. 3). Unlike the flows c–e, most of the cooling in flow f occurs not at the piston, but in the cooling cusp at $r \approx 30$ kpc. Model f resembles model b in having an external cooling flow in $r \gtrsim 30$ kpc that is supported by gas heated by waves that reflect at this impedance barrier.

The impedance barriers in models b and f, where the density and temperature vary significantly over one wavelength, are a long-term result of unrealistically intense central wave heating and are grossly incompatible with observations. However, long before impedance barriers appear in the solutions, as shown in Figure 4, the temperature and density structure of the hot gas has evolved far from typically observed profiles. In principle the hot central cores in these models could be smoothed by outward thermal conduction, but this is irrelevant, since in observed clusters the inner temperature gradient is positive and the conduction, if it were important, should be heating the central gas, not cooling it. The sharp positive density jump in models b and f are very likely to be disrupted by Rayleigh-Taylor (RT) instabilities. However, in our previous two-dimensional calculations, in which the RT instability was allowed to develop naturally, we show that including

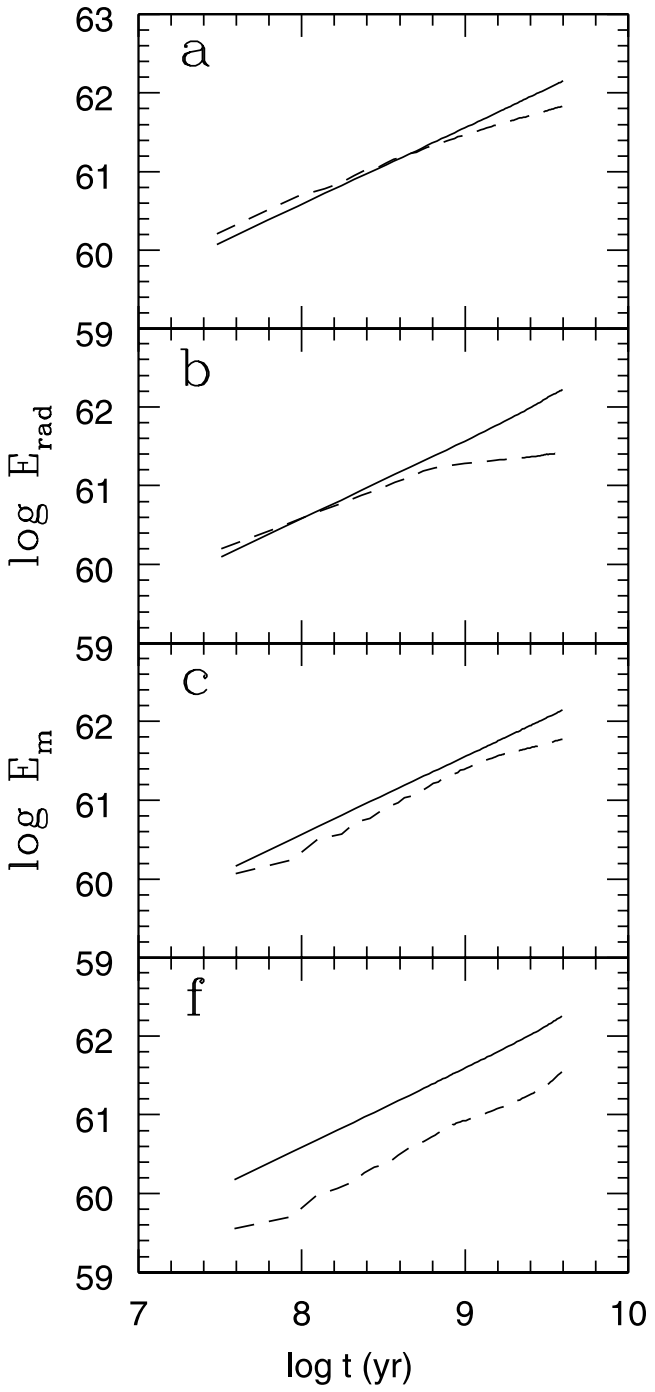

FIG. 5.—Total amount of mechanical energy $E_m(t)$ delivered to the Perseus gas by the spherical piston after time t (*dashed lines*) for flow models a–c and f compared to the total bolometric energy lost in radiation $E_{\rm rad}(t)$ (*solid lines*), both in ergs.

more computational dimensions does not avoid the problems associated with the wave-heating hypothesis (Brighenti & Mathews 2003). All centrally heated flows we considered (allowing for RT) resulted in $dT/dr < 0$, in violation of CR2.

6. SUMMARY AND CONCLUSIONS

Following the discovery of shock ripples in the Perseus and Virgo Clusters, it has often been assumed that this is the fundamental global heating mechanism that prevents the gas from cooling as required by X-ray spectral observations. A heating process can dynamically shut down a cooling flow if it distributes enough energy to reduce or reverse the small negative flow velocity out to approximately the cooling radius. It is clear that the subsonic formation of large X-ray cavities creates weak shocks that move far out into the flow and that these waves dissipate some of their energy in remote regions of the flow.

Nevertheless, we have demonstrated here that the transport of energy by outwardly propagating waves is not likely to be the dominant process that accounts for the absence of cool and cooling gas in these flows. The main problem with this idea is that the density structure of the hot gas varies as $\rho \propto r^{-s}$, where $s < 2$, so that outgoing waves dissipate most of their energy in the central part of the flow and too little at $r \sim r_{\rm cool}$. The result is that after a few Gyr the gas temperature profile flattens and eventually peaks near the center of the flow, just opposite to observed temperature profiles in cooling-core clusters (e.g., Allen et al. 2001), violating the second cardinal requirement (CR2). Much enthusiasm for ripple heating has resulted from calculations that proceeded for only $\sim$0.3 Gyr (e.g., Ruszkowski et al. 2004a, 2004b), as in our model a1, but we have shown here that the temperature profile deteriorates on more relevant Gyr timescales. In a similar calculation Dalla Vecchia et al. (2004) describe wave-heated flows and compute to 1.5–5 Gyr, but find, as we do, that the resulting temperature profile differs from those observed.

Very recently, after this paper was submitted, Fujita & Suzuki (2005) presented a model of steady state cluster gas heating with weak shocks that reproduces many of the same results derived here. In particular, they find that a series of weak shocks propagating out in the Perseus Cluster results in unrealistically strong heating in the core.

The unsatisfactory results described here are similar to the difficulties we encountered in our earlier explorations of cooling flows that were heated in a variety of ways (Brighenti & Mathews 2002a, 2003). Our centrally heated cooling flows produced rising bubbles and weak shocks that propagated to large radii, but we did not discuss distant wave dissipation in detail. We also found that (feedback) heating the central regions of cooling flows often simply moved the cooling to larger radii, but did not diminish the cooling rate (as in the ripple-heated models b and f described here). Large-scale cooling inflow can be stopped if the AGN feedback heating is rapid, extends to $\sim r_{\rm cool}$, and is supplemented by thermal conduction from large radii (Ruszkowski & Begelman 2002), but the amount that thermal conduction is suppressed by magnetic fields needs some fine-tuning (Brighenti & Mathews 2003). A similar unphysical fine-tuning is apparent in the wave-heated models described here—the location, amplitude, and period of wave creation by the X-ray cavities must be finely and unrealistically regulated to ensure just the proper amount of heating in distant regions of the flow to balance radiative losses, i.e., $E_m \sim E_{\rm rad}$, although the resulting temperature gradient is unacceptable.

Most of this fine-tuning can be avoided if both mass and energy are redistributed outward in the hot gas as in the circulation flows described by Mathews et al. (2003, 2004). In these flows the mass transported by dense inflowing gas is balanced by a nearly equal amount of gas flowing outward to large radii carrying both mass and energy. The denser inflow emits most of the radiation and appears as a normal cooling flow with a temperature profile that matches the observations. Meanwhile, bubbles of hot gas heated by the central AGN flow out rapidly and contribute much less to the overall X-ray emission. Our previous two-dimensional computational models of heated flows lacked the spatial resolution to isolate individually rising bubbles as they move large distances upstream through the denser gas, but circulation flows can be computed in a more schematic fashion

(Mathews et al. 2004). In mass-circulating flows it is only necessary that gas near the central AGN be heated sufficiently to have an entropy similar to gas at approximately $r_{\rm cool}$ or beyond. The best argument for outward mass circulation is the vast regions of iron-enriched gas that extend far beyond the stars in the central galaxy, where the iron is produced.

We argue here that neither the PV work done as the hot X-ray cavities inflate or viscous heating by cavity-driven turbulence is a strong source of local heating; this is consistent with the low gas temperatures observed in cooling-core clusters in the central region where bubbles are observed. This suggests that the AGN energy (and mass) must be distributed nonlocally to more distant gas.

To summarize, we have shown that viscous dissipation in outwardly propagating weak shock waves cannot keep the gas in the Perseus Cluster from cooling without heating the gas in the central regions far above the observed temperatures. Since weak shocks have been observed in Perseus and elsewhere, some heating is expected, but they are not the dominant heating mechanism. The shocks observed are almost certainly produced by the subsonic inflation of X-ray cavities, which, as we have shown, produce nonlinear waves that rapidly steepen into weak shocks. Evidently, cavity-produced shocks are too infrequent or weak to generate mechanical luminosities comparable to the X-ray losses.

Studies of the evolution of hot gas in elliptical galaxies at UC Santa Cruz are supported by NASA grants NAG 5-8409 and ATP02-0122-0079 and NSF grants AST-9802994 and AST-0098351, for which we are very grateful.

REFERENCES

Allen, S. W., Schmidt, R. W., & Fabian, A. C. 2001, MNRAS, 328, L37
Begelman, M. C. 2001, in ASP Conf. Ser. 250, Particles and Fields in Radio Galaxies Conference, ed. R. A. Laing & K. M. Blundell (San Francisco: ASP), 443
Bettoni, D., Falomo, R., Fasano, G., & Govoni, F. 2003, A&A, 399, 869
Birzan, L., Rafferty, D. A., McNamara, B. R., Wise, M. W., & Nulsen, P. E. J. 2004, ApJ, 607, 800
Böhringer, H., Matsushita, K., Churazov, E., Ikebe, Y., & Chen, Y. 2002, A&A, 382, 804
Braginskii, S. L. 1958, Soviet Phys.—JETP Lett., 6, 358
Brighenti, F., & Mathews, W. G. 2002a, ApJ, 573, 542
———. 2002b, ApJ, 574, L11
———. 2003, ApJ, 587, 580
Brüggen, M. 2003, ApJ, 592, 839
Brüggen, M., & Kaiser, C. R. 2002, Nature, 418, 301
Brüggen, M., Kaiser, C. R., Chruazov, E., & Ensslin, T. A. 2002, MNRAS, 331, 545
Churazov, E., Brüggen, M., Kaiser, C. R., Böhringer, H., & Forman, W. 2001, ApJ, 554, 261
Churazov, E., Forman, W., Jones, C., Sunyaev, R., & Böhringer, H. 2004, MNRAS, 347, 29
Churazov, E., Sunyaev, R., Forman, W., & Böhringer, H. 2002, MNRAS, 332, 729
Clarke, T. E., Sarazin, C. L., Blanton, E. L., Neumann, D. M., & Kassim, N. E. 2005, ApJ, 625, 748
Conselice, C. J., Gallagher, J. S., III, & Wyse, R. F. G. 2001, AJ, 122, 2281
Dalla Vecchia, C., Bower, R. G., Theuns, T., Balogh, M. L., Mazzotta, P., & Frenk, C. S. 2004, MNRAS, 355, 995
De Grandi, S., Ettori, S., Longhetti, M., & Molendi, S. 2004, A&A, 419, 7
De Grandi, S., & Molendi, S. 2002, ApJ, 567, 163
Faber, S. M., et al. 1997, AJ, 114, 1771
Fabian, A. C., Reynolds, C. S., Taylor, G. B., & Dunn, R. J. H. 2005, MNRAS, 363, 891
Fabian, A. C., Sanders, J. S., Allen, S. W., Crawford, C. S., Iwasawa, K., Johnstone, R. M., Schmidt, R. W., & Taylor, G. B. 2003, MNRAS, 344, L43
Forman, W., et al. 2003, preprint (astro-ph/0312576)
Fujita, Y., & Suzuki, T. K. 2005, ApJ, 630, L1
Kaiser, C. R., & Binney, J. 2003, MNRAS, 338, 837
Kinsler, L. E., Frey, A. R., Coppens, A. B., & Sanders, J. V. 2000, Fundamentals of Acoustics (4th ed.; Wiley: New York)
Mathews, W. G., & Brighenti, F. 2003, ARA&A, 41, 191
Mathews, W. G., Brighenti, F., & Buote, D. A. 2004, ApJ, 615, 662
Mathews, W. G., Brighenti, F., Boute, D. A., & Lewis, A. D. 2003, ApJ, 596, 159
Mathews, W. G., Buote, D. A., & Brighenti, F. 2001, ApJ, 550, L31
O'Sullivan, E., Vrtilek, J. M., Kempner, J. C., David, L. P., & Houck, J. C. 2005, MNRAS, 357, 1134
Peres, C. B., Fabian, A. C., Edge, A. C., Allen, S. W., Johnstone, R. M., & White, D. A. 1998, MNRAS, 298, 416
Peterson, J. R., et al. 2001, A&A, 365, L104
Prestwich, A. H., Joy, M., Luginbuhl, C. B., Sulkanen, M., & Newberry, M. 1997, ApJ, 477, 144
Quilis, V., Bower, R. G., & Balogh, M. L. 2001, MNRAS, 328, 1091
Ruszkowski, M., & Begelman, M. C. 2002, ApJ, 581, 223
Ruszkowski, M., Brüggen, M., & Begelman, M. C. 2004a, ApJ, 611, 158
———. 2004b, ApJ, 615, 675
Sanders, J. S., Fabian, A. C., Allen, S. W., & Schmidt, R. W. 2004, MNRAS, 349, 952
Soker, N., White, R. E., III, David, L. P., & McNamara, B. R. 2001, ApJ, 549, 832
Trujillo, I., Burkert, A., & Bell, E. F. 2004, ApJ, 600, L39
Voigt, L. M., & Fabian, A. C. 2004, MNRAS, 347, 1130